JJEES

JJEES (2026) 17 (3): 351-363
ISSN 1995-6681

Jordan Journal of Earth and Environmental Sciences

A Geospatial Analysis of Coal Mining-Induced Land Use Transformation in the Saleki Reserve Forest, Assam, India

Shyamal Borah* and Monjit Borthakur

Department of Geography, Cotton University, Guwahati, India

Received on 23 June 2025, Accepted on 29 April 2026

Abstract

This study employed supervised classification using multi-temporal ResourceSat imagery (2012, 2018, and 2024) to map land use and land cover (LU/LC) changes in the Saleki Reserve Forest, achieving high overall accuracy (94–96%) and QADI values of 0.06, 0.0283, and 0.0447, respectively. Despite some misclassifications among spectrally similar classes (e.g., built-up, mining, and barren land). The results revealed a substantial increase in coal mining, with mining area expanding by 396 ha (189%), including key hotspots, such as the 4-sq-mile lease (+77.4%) and Tirap grant (+54.7%), while the Ledo OCP area declined by 60.7%. This expansion coincided with a 16.5% loss in forest cover, a 303.8% rise in bare land, and a 40.9% reduction in water bodies. The Landscape Transformation Index rose significantly from 14.7 (2012–2018) to 38.6 (2012–2024), indicating intensified anthropogenic pressure. Canopy density analysis (2018–2024) revealed regeneration in some degraded areas, and forest cover density over trends 12 years highlighted partial conservation success. Overall, the findings emphasize the conflict between mining-driven deforestation and ecosystem resilience, underlining the need for integrated land-use planning, legal enforcement, and sustainable mining. A key limitation was the exclusive use of visible-band data, affecting class separability.

Keywords: *Coal mining, land use/ land cover, forest degradation, forest cover density, Makum Coalfields, Saleki*

1. Introduction

The land use (LU) is defined as human activity taking place on land; and the land cover (LC) is defined as the physical substance that is on or above (in the case of vegetation) the Earth's surface (Chang et al., 2018; Comber et al., 2005; Nedd et al., 2021; Pandey et al., 2021; Trautwein and Pletterbauer, 2018). Land use/land cover (LU/LC) change is now a focal point of environmental monitoring and natural resource management due to the rigid relationship between LU/LC change, anthropogenic changes, and ecosystem processes (Abusmier and Al-Kofahi, 2025; Akhtar et al., 2025; Mishra et al., 2020)particularly in developing countries, where cities generally lack adequate planning. Nowadays, the majority of Jordan's population lives in cities. Zarqa governorate is among the most populated governorates in Jordan and is located within the boundaries of a major hydrological basin. Therefore, the objectives of this study were to explore the spatial and temporal varying dynamics in the urban area and agricultural areas over the past two decades (2001-2021. Several factors are influencing LU/LC, like urbanization, climate change, and land conversion (Fitriani et al., 2025; Okoduwa et al., 2025). Still, very uniquely, mining activities have caused compounding limits to LU/LC globally, resulting in deforestation, loss of biodiversity, and environmental collapse as shown in Odisha (M. Mishra et al., 2022), Cameroon (Tamfuh et al., 2024), Ghana (Gbedzi et al., 2022), Rwanda (Niyonsenga and Sibomana, 2024), Bangladesh, Mongolia (Guan et al., 2017), Germany, and China's Loess Plateau (Cioc, 1998; Lin et al., 2021). In India, coal mining has forced profound LU/LC changes in Ramagundam (Kiran et al., 2022), Godavari (Garai and Narayana, 2018), Singrauli (Khan and Javed, 2012), Jharhia (Uddin Siddiqui and Kumar Jain, 2022), and Raniganj (Patra et al., 2022)India. Owing to its multifaceted consequences on soil, water, and landholders, assessment of spatio-temporal changes in mining areas has become important. The oldest coal mine of India, Raniganj coalfield has been producing superior quality non-coking coal for the last 246 years. To reduce the cost per unit production of coal, the mining authority prefers the opencast method over underground mining. The mushrooming growth of opencast mines in this coalfield causing huge waste dumps, depletion of vegetated surface, changing slope and drainage pattern, soil erosion, and degradation of environmental quality. With this background, the present study examines the spatio-temporal changes and evolution of opencast mines using multi-temporal Landsat Thematic Mapper (TM resulting in dramatic loss of vegetation and forest.

LU/LC transformations, caused by mining, negatively impact forest canopy density (FCD), which reflects the composition, structure, and preservation levels of forests about ecosystem stability. Research has demonstrated that canopy cover has been drastically diminished, with the canopy code at some mining sites dropping from >80% cover to <30% (Galiatsatos et al., 2020; Liu et al., 2024)reporting and verification (MRV. Similar declines in canopy density occurred in Indian states that are major coal producers, such as Jharkhand, Odisha, Chhattisgarh, and Madhya Pradesh (Joshi et al., 2006; Khan and Javed, 2012; Mohanty et al., 2020; Thakur et al., 2022). Compensatory afforestation has

* Corresponding author e-mail: shyamalborahsb106@gmail.com

not been able to fully restore canopy cover to levels recorded before the forest was cleared, due to limits imposed at each site by soil, species selections, and ecological suitability. In this context, socio-ecological systems that depend on forests for sustainable livelihoods further contribute to instability and fragility (López-Bedoya et al., 2022). In the coalfields of Assam, there are indications that mining expanded by 194 ha between 2000 and 2020, leading to growing problems with acid mine drainage, heavy metal leaching, and soil erosion (Kumar et al., 2023; Yadav et al., 2018). The North Eastern Coalfield (NEC), a unit of Coal India Limited, has produced or delivered an estimated 13.68 million tons of coal between 2003 and 2021, across 9 Mining Leases, totaling 5,377.82 ha since the NEC sale of coal began (Katakey, 2021).

The Saleki Reserve Forest (RF) in the Makum coalfields faces the threat of mining encroachment due to increased mining activity. There are currently six active mining leases within Saleki RF, equaling 1,308.22 ha of land, namely, 4 sq. mile (1032.27), 4.48 Sq. Mile (4.97), Tirap Coal Grant (27.28 ha), Namdang Coal Grant (150.24 ha), Ledo OCP (27.06 ha), and Tikok OCP (67.47 ha), with the current leases running from 2023 to 2029. Mining activity within the Reserve Forest entailed occupation within a reserve forest of 183 ha in 2003, to 1043.2 ha in 2020; and mining activities not inside the reserve increased from 9 ha in 2003 to 415.6 in 2020. Mining areas totaled 192 ha in 2003 and increased to 1,458.8 ha in 2020. Within this same time frame, opencast mining has increased in area from 192 ha in 2003 to 479.1 ha in 2020, rat-hole mining increased in area from 0 ha in 2003 to 979.7 ha in 2020 (Katakey, 2021). Even though many studies have documented LU/LC changes in coal mining regions, there is little spatiotemporal analysis of protected reserve forests such as the Saleki RF, where fragile ecosystems are threatened by rapid, localized degradation from opencast and rat-hole coal mining. The current study serves to address this by assessing LU/LC and FCD spatial-temporal changes in Saleki RF from 2012 to 2012, in the context of the Ledo OCP, 4 Sq. Mile lease, and Tirap Coal Grant, using geospatial tools to synoptically assess the ecological consequences of continued expansion and exploitation of coal resources.

2. Study Area and Methodology

2.1 Study area

Saleki Reserve Forest is a part of the Dehing Patkai Elephant Reserve located in Tinsukia District in Assam (Figure 1). It has an area of approximately 40 sq km (27°15′N to 24°19′ N latitudes 95°42′E to 95°49′E longitudes). It was proposed as a reserve forest in 1976 and was notified on the 9 March, 2022. The reserve forest is situated within the Namdang coal grant and the Tikok open-cast project, while the Ledo open-cast project and the Tirap coal grant are located to the east. Total annual rainfall exceeds 4,000 mm and it is often the highest in the month of June. The climatic means are generally between 6 and 38°C. Structural hills with elevations between 143-492 meters characterize the area; there are approximately 119-164 days of rain in a year with a prolonged drier season from October to February.

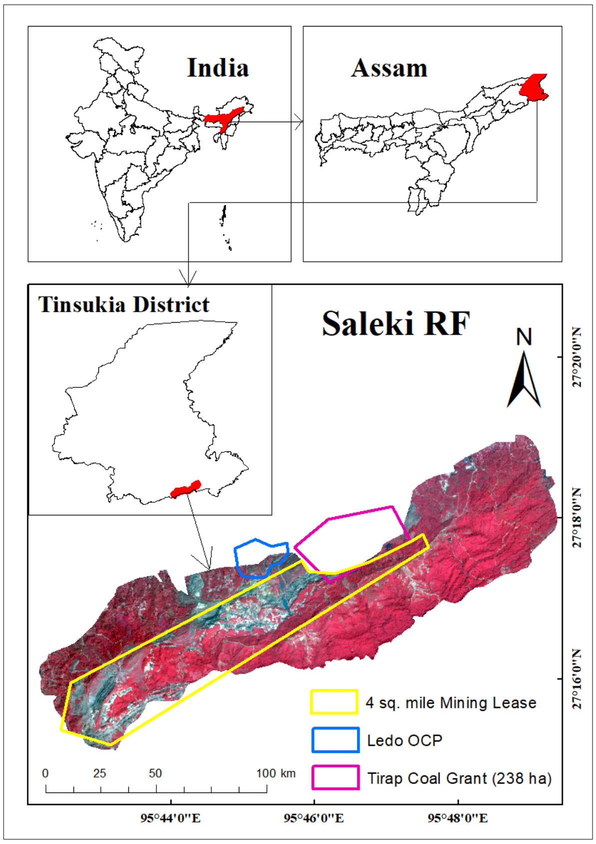

Figure 1. The Saleki RF is indicated in false color composite (LISS-4,8th March 2024)

2.2 Data collection and sources

The present study employed ResourceSat LISS-4 sensor data for LU/LC pattern analyses, utilizing specific datasets (Table 1). Focusing on the recent decade (2012-2024), the study investigated extensive mining activities in the region. The corresponding satellite datasets were obtained from Bhuvan's Bhoonidhi, ISRO's Earth Observation (EO) data hub.

Table 1. Details of satellite data

Acquisition Date	Satellite	Sensor	Path/row	Spatial resolution (m)	Source
01-11-2012	ResourceSat-2	LISS-4	114/052	5	NRSC
04-04-2018	ResourceSat-2A	LISS-4	114/052	5	NRSC
08-03-2024	ResourceSat-2A	LISS-4	114/052	5	NRSC

Source: Authors

Due to the limited spatial extent of the Saleki RF, high-resolution satellite data are essential for precise land use/ land cover study. However, high-resolution LISS-4 sensor databases have only been available from 2012 onward for this specific location. To supplement the analysis and validate LU/LC statistics, this study relied on the following secondary data sources:

- The Report of the 'One Man Commission of

Inquiry' (Vol. I & II) by Brojendra Prasad Katakey, published on April 7, 2021, by the Assam State Government.

- Relevant existing literature, including:

  - Newspaper articles

  - Journal articles

These secondary sources provide valuable context and insights to support the primary satellite data analysis.

2.3 Methodology

2.3.1 Land use/land cover classification

The current study's workflow includes satellite data acquisition, image preprocessing, image classification, accuracy assessment, change-detection analysis, and forest canopy density mapping (Figure 2). A supervised classification method was employed to classify satellite images. The following sections provide extensive explanations of the various steps.

Image pre-processing and classification

The necessary image pre-processing was performed on the data for the three specified years (2012, 2018, and 2024). Image pre-processing, classification and analysis were conducted using Geospatial software (ERDAS Imagine and ArcGIS). Supervised image classification (maximum likelihood method) was performed in ERDAS Imagine. To identify the changes, images were broadly classified into five categories: built-up area, mining, forest area, bare land and water body (Table 2). Training samples for supervised classification were selected using a combination of high-resolution Google Earth imagery and field observations. Mining areas were identified based on characteristic features such as excavation pits, overburden dumps, and haul roads, distinguishing them from non-mining open land. Only spectrally homogeneous and clearly identifiable areas were used as training data to minimize misclassification in LISS-4 imagery.

Table 2. Land use Classification scheme

Sl. No	Class name	Description
1	Water body	Reservoirs, rivers, open water, ponds, etc.
2	Mining	Coal mines, abandoned mines, dumped yards, etc.
3	Forest area	Dense forest and open forest.
4	Bare land	Exposed soils, barren area, etc.
5	Built-up area	Residential, commercial, transportation, roads, pavements, etc.

Accuracy assessment

The Ground Truth Points (GTPs) were selected independently from training samples and were evenly distributed across the study area. They were derived from field observations and high-resolution Google Earth imagery, including both homogeneous and mixed pixels rather than only pure pixels. This ensured independent and unbiased accuracy assessment. The accuracy assessment methods include the standard Kappa coefficient, overall accuracy, producer's accuracy and user's accuracy. Overall accuracy indicates the number of pixels that are properly identified. The frequency of occurrence of a map class on the ground is determined by the user's accuracy. The producer's accuracy indicates the number of classified pixels in a class that accurately fits into that class. Equation 1 shows estimations for accurate Kappa statistics for the stratified random.

$$\text{Kappa coefficient} = (T \times C) - G/T2 - G \quad (1)$$

(Arumugam et al., 2021; Vieira et al., 2010)

Where T is the test pixels, C is the correctly classified pixels observations and G is the sum of the multiplied total value.

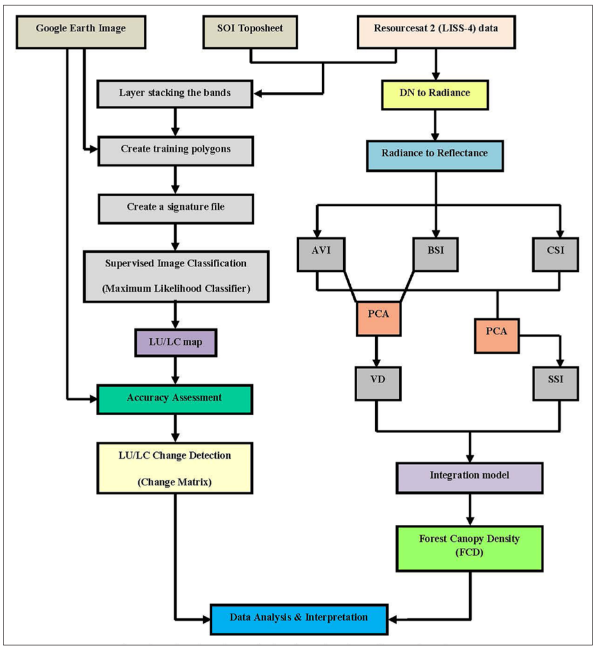

Figure 2. Flowchart showing the methods adopted to determine LU/LC change

The overall accuracy is calculated by dividing the sum of the values along the major diagonal by the total number of reference pixels (Equation 2). The traditional accuracy assessment methods included the standard Kappa coefficient followed by the overall accuracy equation, producer's accuracy and user's accuracy as indicated in equations 3 and 4 (Arumugam et al., 2021).

$$Overall\ Accuracy = (1/N) \sum_{i=1}^{r} n_{ii} \quad (2)$$

$$Producer's\ Accuracy = (n_{ii}/n_{icol}) \quad (3)$$

$$User's\ Accuracy = (n\_ii/n\_irow) \quad (4)$$

Where n_{ii} is the number of suitably classified pixels, N is the total number of pixels; r is the number of rows, n_{icol} is the column total, and n_{irow} is the row total.

Quantity and Allocation Disagreement Index (QADI): This index calculates the degree of disagreement between the classification results and reference maps by keeping incorrectly labeled pixels as A and the difference in the pixel count (for each class) between the classified map and reference data as Q (Feizizadeh et al., 2022)various alternative measures have been investigated with minimal success in practice. In this article, we introduce a novel index that overcomes the limitations. Unlike Kappa, it is not sensitive to asymmetric distributions. The quantity and allocation disagreement index (QADI. The QADI index, which measures the degree of disagreement and variation, is then calculated from these values. Additionally, it can be used to create a graph showing how much each component contributes to the disagreement (Feizizadeh et al., 2022) various alternative measures have been investigated with minimal success in practice. In this article, we introduce a novel index that overcomes the limitations. Unlike Kappa, it is not sensitive to asymmetric distributions. The quantity and allocation disagreement index (QADI. The equation 5 for the QADI index is as follows:

$$QADI = \sqrt{\left(\frac{A}{N}\right)^2 + \left(\frac{Q}{N}\right)^2} \quad (5)$$

The resulting QADI value varies between 0and 1 (Feizizadeh et al., 2022)various alternative measures have been investigated with minimal success in practice. In this article, we introduce a novel index that overcomes the limitations. Unlike Kappa, it is not sensitive to asymmetric distributions. The quantity and allocation disagreement index (QADI.

2.3.2 Forest Canopy Density

Radiometric correction

Radiometric correction takes raw Digital Numbers (DN) and converts them to physical values to accurately represent a surface. Equation 6 shows the steps to convert DN to at-sensor radiance.

$$L\lambda = SR_k/DN_{max} \times DN \quad (6)$$

Where, Lλ: At-sensor spectral radiance ($W/m^2/sr/\mu m$)

SR_k: Saturation radiance for the k^{th} band (provided in metadata)

DN: Digital Number of the pixel

DN_{max}: Maximum possible value of pixel

To obtain at-sensor (TOA) reflectance, radiance values were converted using Equation 7:

$$Rsensor = \frac{L_\lambda \times \pi \times d^2}{E_{sun} \times cos\theta_z} \quad (7)$$

Where pi =3.14159

Rsensor = reflectance at the sensor

L_λ = spectral radiance at the sensor's aperture

E_{sun} = mean solar exo-atmospheric irradiance

θ_z = solar zenith angle

d = Earth-Sun distance

Advanced Vegetation Index (AVI)

The Advanced Vegetation Index (AVI) is a vegetation metric that was developed to increase sensitivity to vegetation density, especially when working in conditions of dense canopy cover, while minimizing the signal from background soil noise. The AVI can be computed using equation 8.

$$AVI = \sqrt[3]{(B4 \times (DN_{max} - B3) \times (B4 - B3) + 1} \quad (8)$$

Bare Soil index (BSI)

The Bare Soil Index (BSI) identifies bare soil areas from satellite imagery. We have provided a simple model of the BSI for LISS-4 in equation 9.

$$BSI = \frac{((B4 + B2) - B3)}{((B4 + B2) + B3} \quad (9)$$

Canopy Shadow Index (CSI)

The Canopy Shadow Index (CSI) identifies shadowed areas beneath dense vegetation canopies, typically indicating healthy forests. The formula for CSI is shown in equation 10.

$$CSI = \sqrt{((DN_{max} - B2) \times (DN_{max} - B3)} \quad (10)$$

To form a Vegetation Density (VD) calculation, we will find Principal Component Analysis (PCA) performance between the AVI and the BSI. Likewise, to form a Scaled Shadow Index (SSI) calculation, PCA will be performed between the CSI and AVI.

Forest Canopy Density

Forest Canopy Density (FCD) is defined as the percentage of land surface area covered by tree canopy in a forested area. One of the equations found in the literature is equation 11.

$$FCD = \sqrt{(VD \times SSI + 1)} - 1 \quad (11)$$

3. Results

3.1 Image classification and accuracy assessment

This study demonstrated the application of supervised classification for LU/LC mapping using multi-year ResourceSat series satellite data. To ensure reliability, accuracy assessments were performed for each year's classified maps using confusion matrices and test samples. The results showed consistent classification accuracy across years, with total accuracy levels of 94% and a Kappa coefficient of 0.86 (2012), 96% and a Kappa coefficient of 0.92 (2018), and 94% and a Kappa coefficient of 0.89 (2024) (Table 3). The producer's accuracy showed that water bodies and mining areas were classified with higher accuracy, while the user's accuracy indicated that water bodies and forest regions were classified with greater correctness. The QADI values for each year were 0.06, 0.02828, and 0.04472, respectively.

Although supervised classification achieved high accuracy, some misclassifications were observed in the classified maps, primarily due to mix-pixel effects, low image resolution, similar surface reflectance, and texture patterns. These misclassifications mostly occurred between built-up areas and mining regions. Accurate classification of coal mining areas, built-up areas, and bare lands using visible-band satellite data is challenging due to their similar spectral properties. However, this limitation can be overcome by utilizing SAR data or microwave satellite data, which offers enhanced feature discrimination based on backscattering intensity and dielectric properties (Forkuor et al., 2020; Ranjan et al., 2021; Ranjan and Parida, 2019). Unfortunately, historical microwave satellite sensor or SAR data are unavailable for this study, precluding its use for change detection.

Despite the difficulty in achieving 100% accuracy in differentiating mining areas from barren land and built-up areas using spectral signatures, the available data can still provide valuable insights for a representative study. Therefore, an analysis of change detection was carried out to recognize the impacts of coal mining activities on LU/LC patterns within the Saleki RF. The LU/LC maps, produced using supervised classification for 2012, 2018, and 2024, are shown in Figure 3.

Table 3. Confusion Matrix of Accuracy Assessment

	Reference Data							
	Class	***B***	***BA***	***W***	***M***	***F***	**Total**	**Au (%)**
	Year – 2012							
Classified Data	***B***	5	0	0	0	1	6	83.33
	BA	0	7	0	0	1	8	87.5
	W	0	0	4	0	0	4	100
	M	0	0	0	7	1	8	87.5
	F	3	0	0	0	71	74	95.94
	Total	8	7	4	7	74	100	
AP (%)	62.5	100	100	100	95.94			
AO (%)	94							
K	0.86201							
QADI	0.06							
	Year – 2018							
Classified Data	***B***	7	0	0	0	0	7	100
	BA	1	11	0	0	0	12	91.66
	W	0	0	3	0	0	3	100
	M	1	0	0	10	2	13	76.92
	F	0	0	0	0	65	65	100
	Total	9	11	3	10	67	100	
AP (%)	77.77	100	100	100	97.01			
AO (%)	96							
K	0.92468							
QADI	0.02828							
	Year – 2024							
Classified Data	***B***	11	1	0	0	3	15	73.33
	BA	1	8	0	0	0	9	88.88
	W	0	0	3	0	0	3	100
	M	0	0	0	10	0	10	100
	F	0	1	0	0	62	63	98.41
	Total	12	10	3	10	65	100	
AP (%)	91.66	80	100	100	95.38			
AO (%)	94							
K	0.89142							
QADI	0.04472							

B Bare land, *BA* Built-up area, *W* Water body, *M* Mining, *F* Forest area, AP the producer's accuracy, Au the user's accuracy, AO the overall accuracy, K = the kappa coefficient, QADI = Quantity and allocation disagreement index

Source: Calculated by the Authors

3.2 LU/LC mapping and change detection analysis of Saleki RF

After calculating the accuracy of prepared LU/LC maps, the areal coverage of each feature was analyzed. The areal coverage of coal mining was 137 ha, 213 ha, and 396 ha for the years 2012, 2018, and 2024, respectively (Table 4). It was observed that the areal coverage of coal mining expanded during 2012–2018, with a 55.47% change rate. However, the rate of increase in mining was recorded at 189.05% during 2012–2024 (Table 5).

A significant decrease rate (-16.48%) was noticed for the forest areas during 2012–2024 (Figure 5). The results show that the change rate of forest area was -8.42% and -8.8% during 2012–2018 and 2018–2024, respectively. The continued loss in forest area coverage suggests that mining activity has a detrimental influence on the forest ecology in the studied region. Moreover, a significant increase in bare land was noticed during 2012–2024 (303.77%). The rate of change in bare land was -1.89%, and 311.53% during 2012–2018 and 2018–2024 respectively. Built-up areas changed a lot over time, going up by 58.4% from 2012 to 2018 and then going down sharply by 77.27% from 2018 to 2024. Permanent settlements are not allowed in this area because it is part of a reserved forest. So, the mapped built-up land is mostly made up of temporary and semi-permanent buildings that coal miners use. These buildings are very close to active mining sites and are left empty or taken down when mining sites move or stop. The decrease in built-up area seen between 2018 and 2024 is due to people moving away from settlements and leaving them behind because of changes in mining activity, not because of planned or stable urban development. Similarly, the area under water bodies has decreased between 2012 and 2024 (-40.91%). The highest LU/LC conversion was in forest area to bare land (285 ha), followed by forest area to coal mining (232 ha) (Table 6). Thus, the lowest conversion was in the mining region to water bodies (0.22 ha). Most of the built-up area has gone back to being bare land (33 ha) and forest (35 ha). Most of the built-up areas are temporary mining labor camps that are left behind when mining shifts or slows down. Structures are taken apart or fall apart, turning into bare land first and then growing back naturally. This explains the change from developed land to forest. Overall, the LU/LC maps revealed that the land coverage of the mining area increased steadily across all classes from 2012 to 2024. As a result of widespread opencast coal mining activities, there has been a large reduction in forest cover, which includes herbs, shrubs and other vegetation (Figure 6). In between the study period, the amount of barren land expanded as well. The bare land consists of exposed soils, desolate areas, etc.

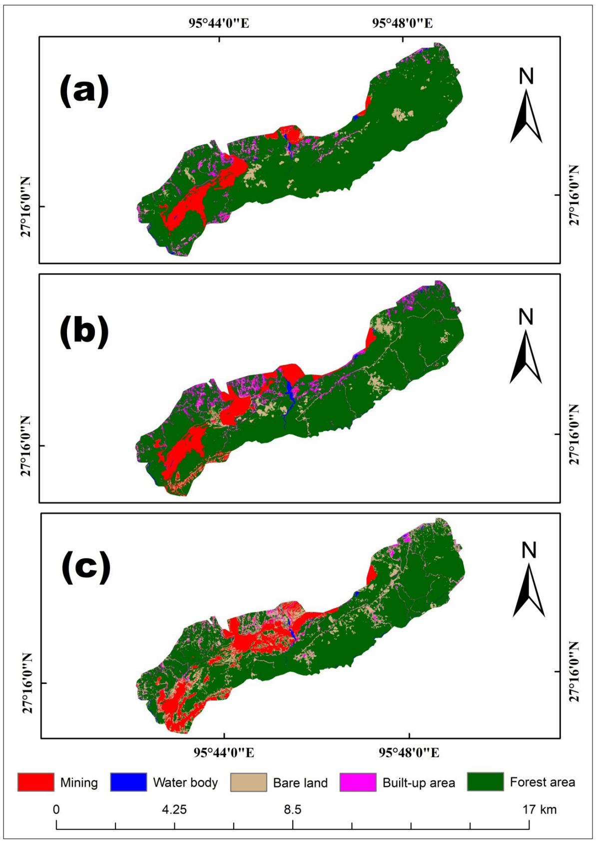

Figure 3. LU/LC map of the Saleki Reserve Forest for the years (a) 2012, (b) 2018, and (c) 2024

Table 4. Areal coverage of LU/LC classes

Year Classes	2012		2018		2024	
	Area (Ha)	Area (%)	Area (Ha)	Area (%)	Area (Ha)	Area (%)
Bare land	106	3.51	104	3.46	428	14.22
Built-up area	250	8.30	396	13.17	90	2.97
Water body	22	0.74	12	0.38	13	0.45
Mining	137	4.55	213	7.06	396	13.15
Forest area	2493	82.86	2283	75.91	2081	69.19
Total Area	3008	100	3008	100	3008	100

Source: Calculated by the Authors

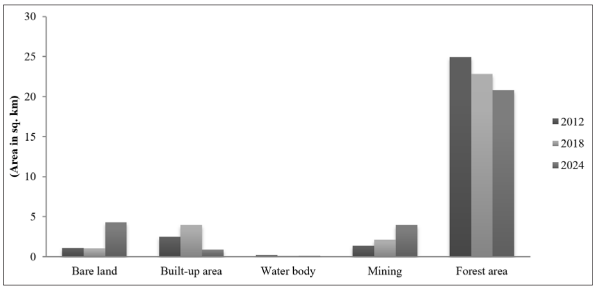

Figure 4. Comparative study of LU/LC change from 2012 to 2024

Table 5. Rate of change in areal coverage of different LU/LC classes

Year/Classes	2012-2018	2018-2024	2012-2024
	Rate of change per year (%)		
Bare land	-1.89	311.53	303.77
Built-up area	58.4	-77.27	-64
Water body	-45.45	8.33	-40.91
Mining	55.47	85.91	189.05
Forest area	-8.42	-8.80	-16.48

Source: Calculated by the Authors

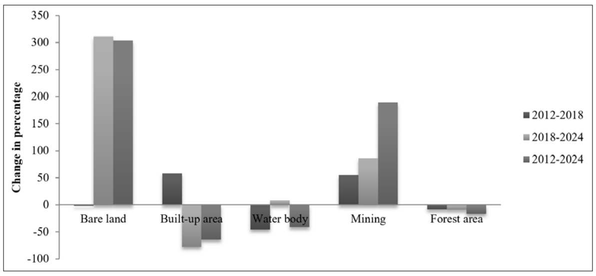

Figure 5. Net change of LU/LC from 2012 to 2024 in percentage

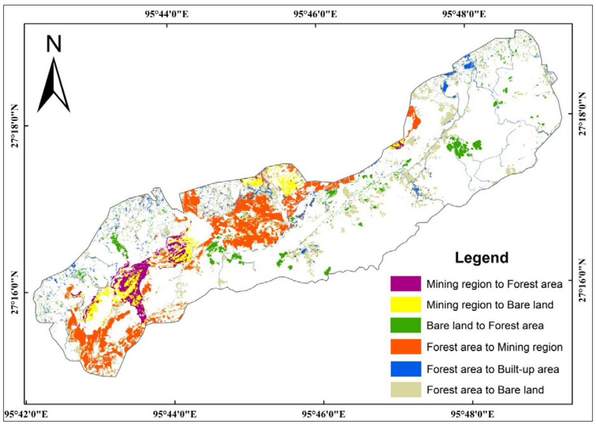

Figure 6. LU/LC conversion map of Saleki RF, 2012 – 2024

Table 6. Transition matrix of LU/LC change in the Saleki RF from 2012 to 2024 (Area in Ha)

Land use/land cover classes	Bare land	Built-up area	Water body	Mining	Forest area	Total in 2024
Bare land	33	7	0.7	24	72	136.7
Built-up area	33	10	0.9	27	35	105.9
Waterbody	2.8	0.8	5	3.6	2.7	14.9
Mining	70	7	0.2	107	57	241.2
Forest area	285	59	6	232	1909	2491
Total in 2012	423.8	83.8	12.8	393.6	2075.7	2989.7

Source: LANDSAT Satellite Image Processing

3.3 Forest Canopy Density in Saleki RF

In this section, changes in forest canopy density within the Saleki Reserve Forest between 2018 and 2024 are examined to assess patterns of forest degradation, regeneration, and broader ecological modification. The analysis focuses on shifts across different canopy density classes to understand spatial and temporal variations in forest condition during the study period. Forest Canopy Density (FCD) maps for the study area were generated using a multi-index approach that integrates the AVI and BSI (Figure 7) and CSI and SSI (Figure 8), each representing distinct biophysical characteristics of vegetation cover and surface conditions.

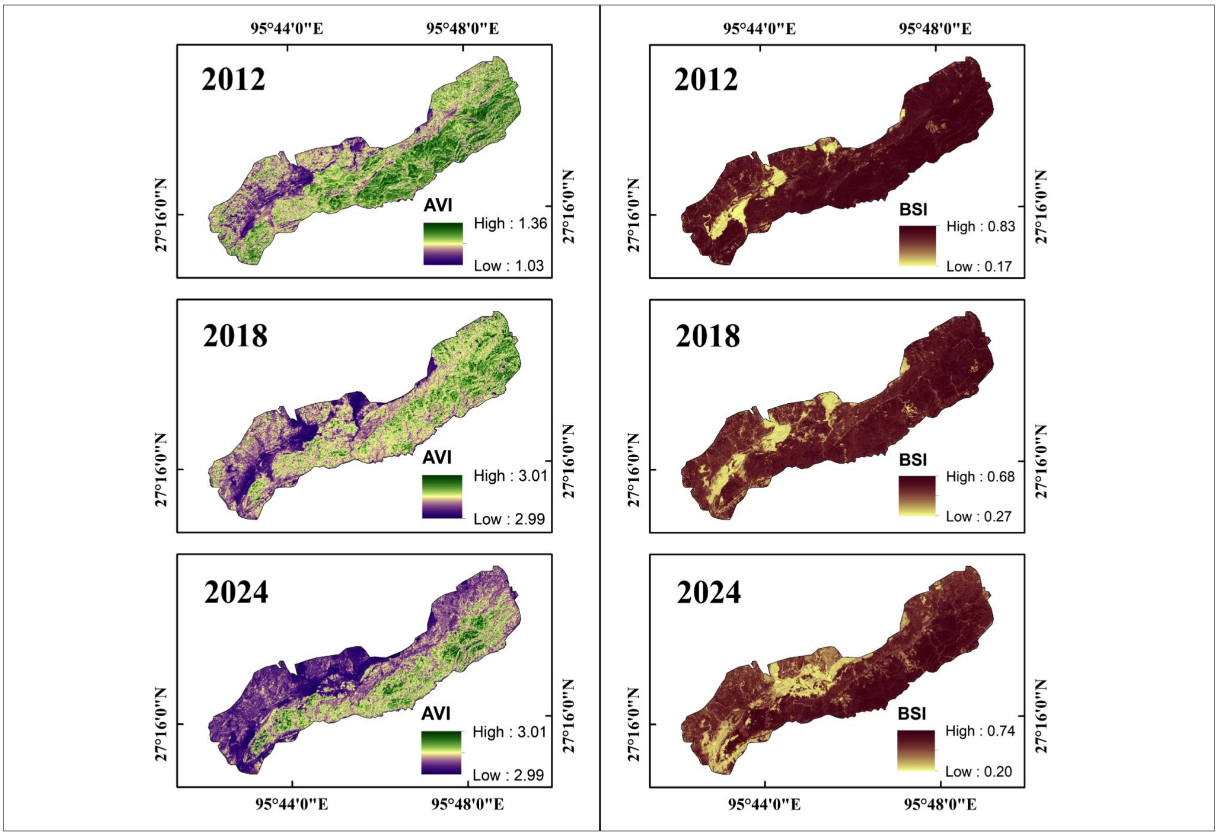

Figure 7. AVI and BSI of Saleki RF

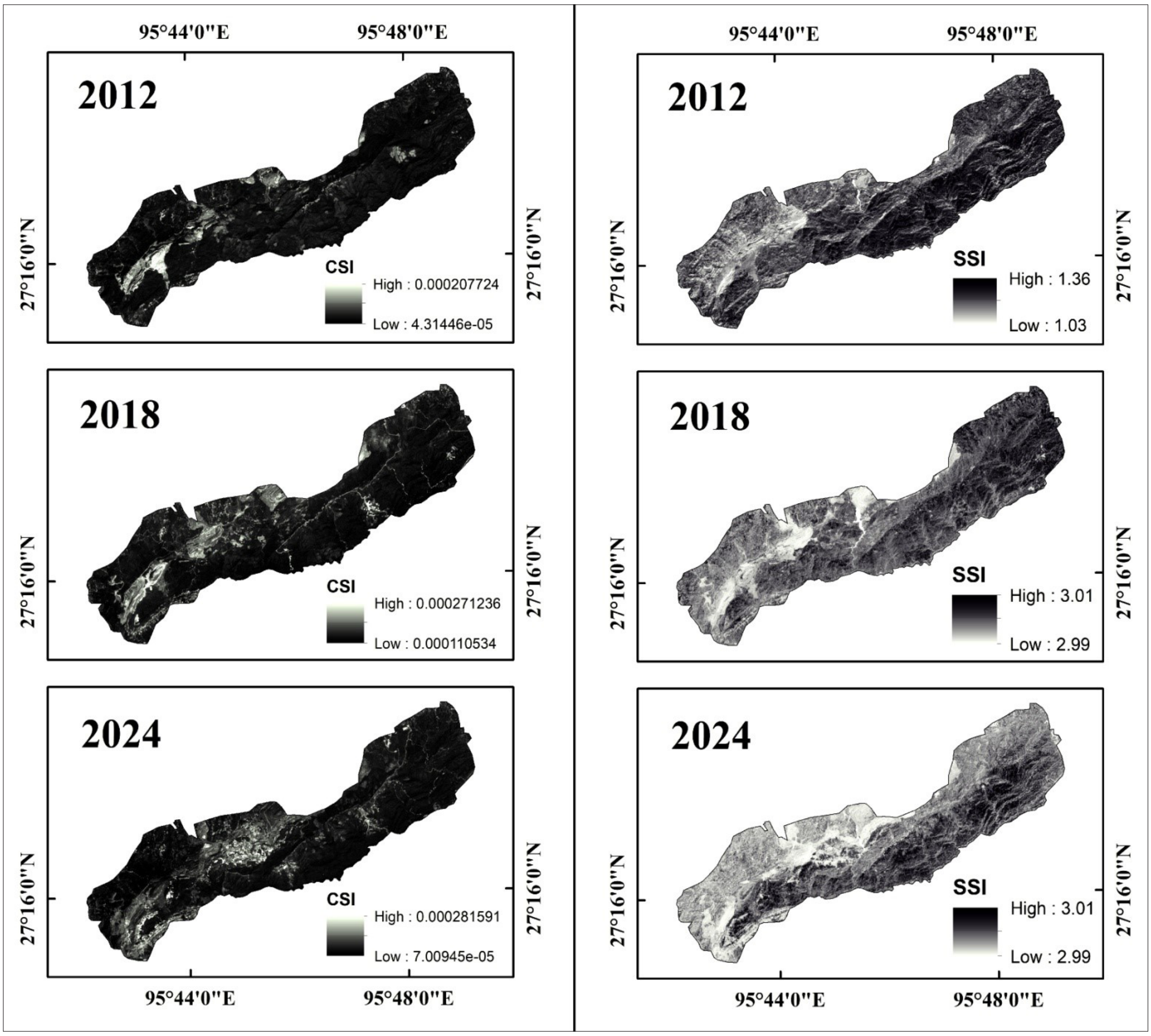

Figure 8. CSI and SSI of Saleki RF

Table 7 indicates the changes in canopy density of forests of Saleki Reserve Forest from 2012 to 2024. In the case of other natural cover like scrub and open forest, it can be concluded that scrub cover has reduced significantly from 1.63 ha to 0.1 ha, Open Forest-I decreased from 31.98 ha to 0.34 ha, and Open Forest-II has decreased sharply from 370.18 ha to 111.67 ha. While Moderately Dense Forest experienced a large decline by 2018, it has had a partial recovery by 2024. Medium Dense Forest increased from 2012 to 2018, then slightly decreased by 2024. The most noticeable cover of Highly Dense Forest has grown 107.12 ha in 2012 to 904.34 in 2024. Therefore, in general, there has been an obvious shift of forest cover density from sparse to denser canopy cover, indicating a successful forest regeneration or conservation efforts. The forest cover density maps for the study area for the year 2012, 2018 and 2024 are available in Figure 9.

Table 7. Category-wise area of Forest Canopy Density in Saleki RF

FCD Classes with FCD in %	2012		2018		2024	
	Area (in ha)	Area (in %)	Area (in ha)	Area (in %)	Area (in ha)	Area (in %)
Scrub land, 0-10	1.6275	0.054	0.02	0.0006	0.1	0.003
Open Forest-I, 11-20	31.9775	1.068	0.5625	0.018	0.3375	0.011
Open Forest-II, 21-40	370.18	12.371	199.84	6.67	111.6675	3.73
Moderately Dense, 41-60	1189.415	39.75	321.18	10.73	522.255	17.45
Medium Dense, 61-80	1291.8925	43.17	1948.69	65.12	1453.5175	48.57
Highly Dense, 81-100	107.1225	3.58	521.9225	17.44	904.335	30.22

Source: Calculated by the Authors

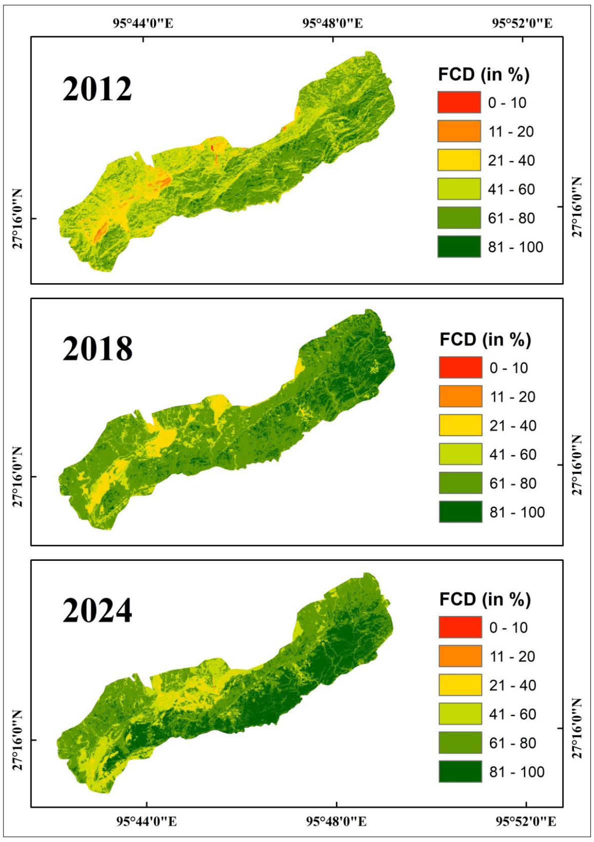

Figure 9. Forest Canopy Density map of Saleki RF

3.4 Expansion of coal mining inside Saleki RF

The unchecked expansion of coal mining activities within the Saleki RF poses a significant threat to its ecosystem. This section examines the spatial-temporal dynamics of coal mining expansion within the forest area. The mining projects inside the Saleki RF; i.e. Ledo Open Cast Project (Ledo OCP), 4 sq. mile mining lease and Tirap coal grant are considered as the critical hotspots of land cover degradation. Figure 10 illustrates the location of these three coal mining projects within the Saleki RF. These projects are overlaid on a false color composite image, providing a visual representation of their spatial distribution within the RF.

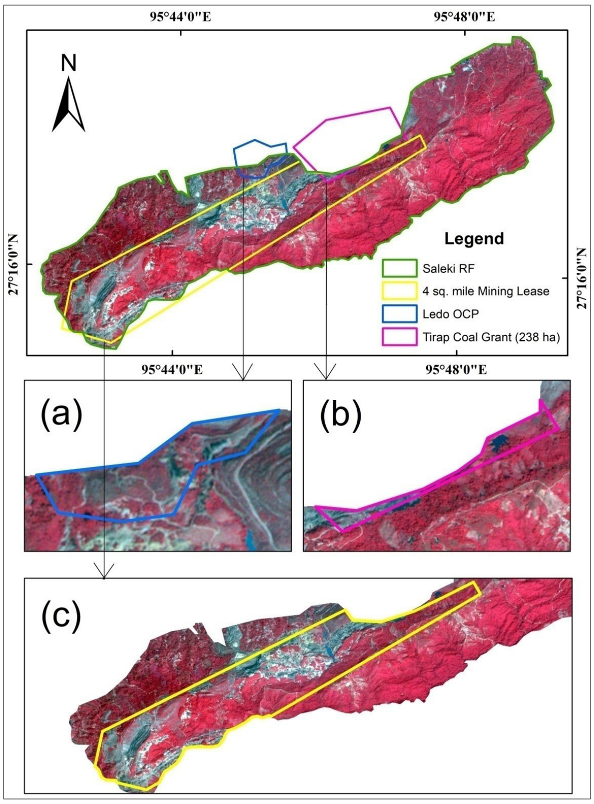

Figure 10. Coal Mining Projects inside Saleki RF, (a) Ledo OCP, (b) Tirap coal grant and (c) 4 sq. mile mining lease are shown in false color composite (LISS-4, dated 8th March 2024)

Table 8. Areal coverage of coal mining inside the Saleki RF in different study years obtained from supervised classification

Name of mining region	2012 (Area in ha)	2018 (Area in ha)	2024 (Area in ha)
Ledo OCP	14.9175	15.7925	5.845
Tirap Coal Grant	5.4525	7.9675	8.44
4 sq. mile mining lease	171.14	229.05	303.4275
Total	191.51	252.81	317.7125

Source: Calculated by the Authors

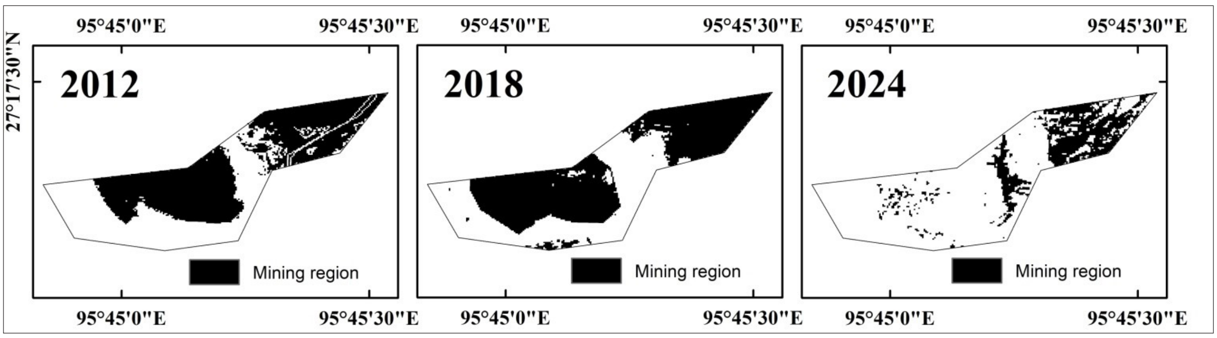

Figure 11. Coal mining region at Ledo OCP inside the Saleki RF in (i) 2012, (ii) 2018, and (iii) 2024

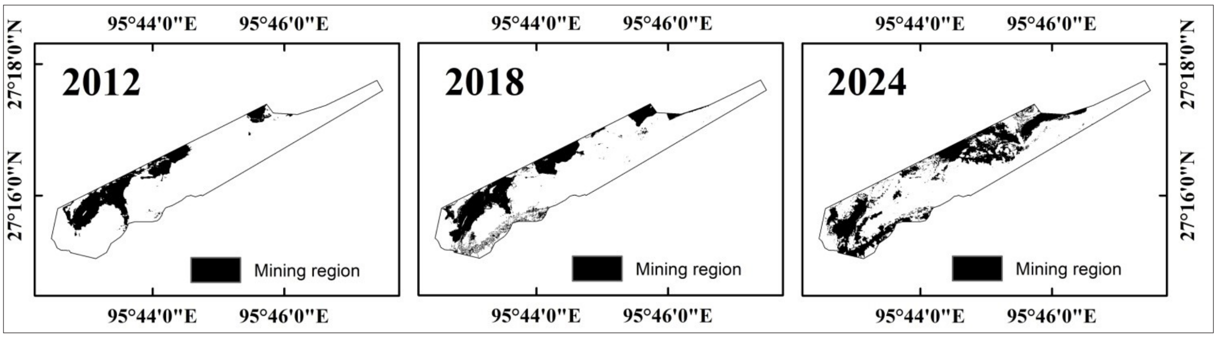

Figure 12. Coal mining region at 4 sq. mile mining lease inside the Saleki RF in (a) 2012, (b) 2018, and (c) 2024

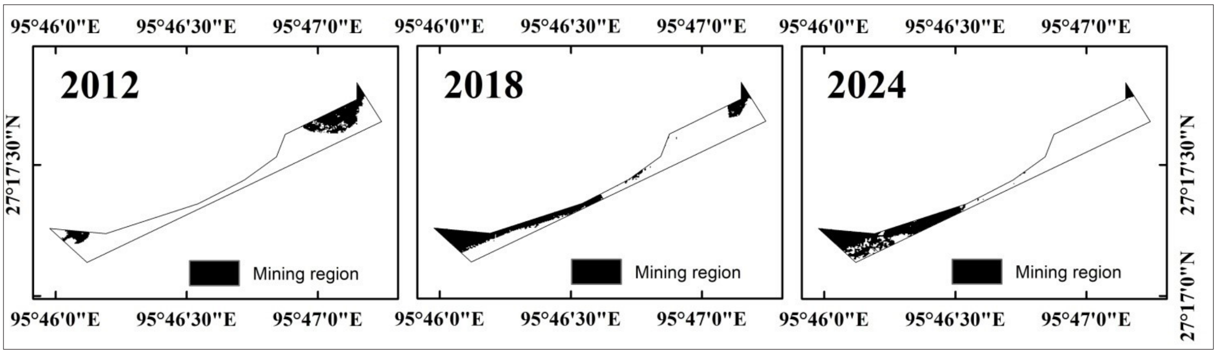

Figure 13. Coal mining region at Tirap coal grant inside the Saleki RF in (a) 2012, (b) 2018, and (c) 2024

The coal mining area inside Saleki RF expanded significantly between 2012 and 2024. The total mining area increased by 66% from 191.51 ha in 2012 to 317.71 ha in 2024 (Table 8). Notably, the 4 sq. mile mining lease registered a 77.4% increase from 171.14 ha to 303.43 ha during this period (Figure 12). Similarly, Coal mining within the Tirap Coal Grant increased by 54.7% from 5.45 ha to 8.44 ha (Figure 13). In contrast, Ledo OCP decreased by 60.7% from 14.92 ha to 5.85 ha (Figure 11). The year-wise increase shows a 32.1% rise from 2012 to 2018 and a 25.6% rise from 2018 to 2024. The three areas are, therefore, considered as the hotspots of coal mining-induced land cover change within the Saleki RF.

3.5 Landscape transformation index of Saleki RF, 201224-

The Landscape Transformation Index (LTI) is a quantitative measure that assesses the magnitude of changes in LU/LC patterns over time. It provides a comprehensive framework for evaluating the degree and nature of landscape transformations, enabling researchers and policymakers to track and understand the dynamics of environmental change (Łowicki, 2008). The LTI is calculated using Equation 12 below:

$$\text{LTI} = (\Sigma|change\ in\ land\ cover\ class|)\ /\ total\ area \tag{12}$$

where Σ of change in land cover class represents the sum of the absolute values of changes in each land cover class and total area represents the total area of the landscape being studied.

- LTI for 2012-2018:

= (|3.51-3.46| + |8.30-13.17| + |0.74-0.38| + |4.55-7.06| + |82.86-75.91|) / 100

= (0.05 + 4.87 + 0.36 + 2.51 + 6.95) / 100

= 14.74

- LTI for 2018-2024:

= (|3.46-14.22| + |13.17-2.97| + |0.38-0.45| + |7.06-13.15| + |75.91-69.19|) / 100

= (10.76 + 10.20 + 0.07 + 6.09 + 6.72) / 100

= 33.84

- LTI for 2012-2024:

= (|3.51-14.22| + |8.30-2.97| + |0.74-0.45| + |4.55-13.15| + |82.86-69.19|) / 100

= (10.71 + 5.33 + 0.29 + 8.60 + 13.67) / 100

= 38.60

The overall change in land cover classes indicates significant changes in the landscape. Bare land increased by 323 hectares (11.71%), while the built-up area decreased by 160 hectares (5.33%). Water bodies experienced a minor decrease by nine hectares (0.29% decrease). Mining areas increased by 259 hectares (8.60%). The forest areas have decreased by 412 hectares (13.67%) from 2012 to 2024. The major changes exemplify a dynamic landscape, which deserves continual monitoring and management of land cover classes to assess their environmental and ecological consequences.

The outputs from the Landscape Transformation Index (LTI) reveal significant changes in the landscape among the three time periods. The LTI values of 14.74, 33.84, and 38.60 during 2012-2018, 2018-2024, and 2012-2024, respectively, show a continuous increase in the landscape transformation within the area. We must note that the net change in land cover classes has resulted in a considerable increase in bare land and mining areas, and a decrease in built-up areas, water bodies, and forest areas.

4. Discussion

The analysis of LU/LC change indicates significant declines in forest cover derived from 2,493 hectares in 2012 to 2,081 hectares in 2024. Simultaneously, mining activity has rapidly and dramatically increased from 137 hectares in 2012 to 396 hectares in 2024. The findings of the present study show that coal mining activities have rapidly destroyed forest cover in Saleki RF during this time. Furthermore, the One Man Commission of Inquiry Report presented by Justice Brojendra Prasad Katakey (Katakey, 2021) supports the majority of these findings by indicating that the extent of encroachment by mining activities is vast in the reserved forest. There has been a similarly alarming trend noted in the BP Katakey report in areas occupied by mining in the reserve forest, which has increased significantly from 183 hectares in 2003 to a shocking 1,043.2 hectares in 2020, with a disproportionate increase from 2018 (474.7 ha) to 2020 (1,043.2 ha). This is suggestive of the significant decreases in tree cover, and increases in mining area established by the study at hand, showing that the encroachment of coal mining is now a consistent trend in underwent encroachment into the reserved forest. Nonetheless, the One Man Commission of Inquiry Report provided an extrapolated estimation on the extent of non-coal mining areas (estimated in hectares) within the reserve forest. Based on the report's classification of mining activity and the estimates, the Environment and Forest Department, Government of Assam, provides a preliminary estimation and has mentioned the need for a scientific study on the issue (Katakey, 2021).

Moreover, the analysis on forest canopy density in the Saleki Reserve Forest offers very an encouraging picture of recovery from 2018 and ending in 2024. The earlier years showed a clear trend of significant degradation, particularly in the open forest and scrub forest classes. The most recent data are very promising, showing high levels of regrowth, primarily in moderately to highly dense forest classes. There was a huge increase in highly dense forest cover across the region, even in the affected mining areas. Mining sites are either demonstrating some success of planned re-growth efforts or significant natural evolution. The recovery of highly dense forest areas and other classes of forest canopy throughout these historically disturbed spaces is promising, since it shows that conservation and rehabilitation strategies have been able to address and reverse the deleterious effects of anthropogenic influences such as mining. Not only that, but increases in forest composition, density, and canopy coverage demonstrate that human-assisted or unassisted forest management efforts can positively contribute to and support equitable transitions towards future ecological stability.

The study results align with existing literature on the impacts of coal mining on forest ecosystems. Studies have consistently shown that coal mining leads to widespread deforestation, habitat destruction, and environmental degradation (Goswami, 2015). The findings of this research also support the notion that the expansion of coal mining and coke coal industries is a significant driver of LU/LC dynamics (A. Mishra et al., 2022). Furthermore, the role of labor migration and settlement expansion in contributing to land cover alteration is consistent with the existing literature (Kutir et al., 2022). However, this study provides new insights into the specific context of Saleki RF, highlighting the need for localized solutions to address the land-use transformations driven by coal mining in this region.

5. Conclusion

This study demonstrates that coal-mining expansion has been a dominant driver of land-use and land-cover transformation in and around the Saleki Reserve Forest, leading to substantial forest degradation, a reduction in water bodies, and an expansion of bare land. Landscape-level indicators confirm continuous and intensifying anthropogenic pressure, particularly in active mining lease areas, while localized declines in some mining zones suggest spatially uneven extraction dynamics. At the same time, recent canopy-density patterns indicate early signs of forest regeneration on degraded lands, highlighting ecological resilience where direct disturbance has slowed. Despite minor spectral limitations in differentiating mining-related land classes, the classification accuracy provides confidence in the observed trends. Overall, the findings underscore the urgent need for integrated land-use planning, stricter enforcement of environmental regulations, adoption of sustainable mining and reclamation practices, and continuous monitoring to balance resource extraction with long-term ecological stability.

Future work can better connect ecological and socio-economic factors and generalize findings by incorporating SAR and multi-temporal data, with site validation within a longitudinal cross-site design.

Statements and Declarations

- Conflict of interest:

The corresponding author declares on behalf of all authors that there is no conflict of interest.

- Funding:

The authors declare that no funds, grants, or other support were received during the preparation of this manuscript.

- Declaration of generative AI and AI-assisted technologies in the writing process:

No AI tools were used in the writing of this work.

References

References

Abusmier, S.A., Al-Kofahi, S.D., 2025. Examining Land Use/Land Cover Dynamics in Zarqa Governorate Major Districts: Implications for Urban and Environmental Sustainability. Jordan J. Earth Environ. Sci. 16, 1–10.

Akhtar, M.M., Khan, T., Khan, A.R., Akhtar, R., Raza, D., 2025. Assessing the Land Use/Land Cover and Climatic Changes Impacts on Static Groundwater Level: A Case Study of Quetta, Pakistan. Jordan J. Earth Environ. Sci. 16, 136–143.

Arumugam, T., Yadav, R.L., Kinattinkara, S., 2021. Assessment and Predicting of LULC by Kappa Analysis and CA Markov model using RS and GIS Techniques in Udham Singh Nagar District, India. https://doi.org/10.21203/rs.3.rs-141832/v1

Chang, Y., Hou, K., Li, X., Zhang, Y., Chen, P., 2018. Review of Land Use and Land Cover Change research progress. IOP Conf. Ser. Earth Environ. Sci. 113, 012087. https://doi.org/10.1088/1755-1315/113/1/012087

Cioc, M., 1998. The Impact of the Coal Age on the German Environment: A Review of the Historical Literature. Environ. Hist. Camb. 4, 105–124. https://doi.org/10.3197/096734098779555754

Comber, A., Fisher, P., Wadsworth, R., 2005. What is Land Cover? Environ. Plan. B Plan. Des. 32, 199–209. https://doi.org/10.1068/b31135

Feizizadeh, B., Darabi, S., Blaschke, T., Lakes, T., 2022. QADI as a New Method and Alternative to Kappa for Accuracy Assessment of Remote Sensing-Based Image Classification. Sensors 22, 4506. https://doi.org/10.3390/s22124506

Fitriani, Y., Abdullah, N., Ridwan, I., 2025. Spatiotemporal Analysis of Wetland Environmental Changes Using Machine Learning and Remote Sensing Data. Jordan J. Earth Environ. Sci. 16, 418–432.

Forkuor, G., Ullmann, T., Griesbeck, M., 2020. Mapping and Monitoring Small-Scale Mining Activities in Ghana using Sentinel-1 Time Series (2015–2019). Remote Sens. 12, 911. https://doi.org/10.3390/rs12060911

Galiatsatos, N., Donoghue, D.N.M., Watt, P., Bholanath, P., Pickering, J., Hansen, M.C., Mahmood, A.R.J., 2020. An Assessment of Global Forest Change Datasets for National Forest Monitoring and Reporting. Remote Sens. 12, 1790. https://doi.org/10.3390/rs12111790

Garai, D., Narayana, A.C., 2018. Land use/land cover changes in the mining area of Godavari coal fields of southern India. Egypt. J. Remote Sens. Sp. Sci. 21, 375–381. https://doi.org/10.1016/j.ejrs.2018.01.002

Gbedzi, D.D., Ofosu, E.A., Mortey, E.M., Obiri-Yeboah, A., Nyantakyi, E.K., Siabi, E.K., Abdallah, F., Domfeh, M.K., Amankwah-Minkah, A., 2022. Impact of mining on land use land cover change and water quality in the Asutifi North District of Ghana, West Africa. Environ. Challenges 6, 100441. https://doi.org/10.1016/j.envc.2022.100441

Goswami, S., 2015. Impact of Coal Mining on Environment. Eur. Res. 92, 185–196. https://doi.org/10.13187/er.2015.92.185

Guan, C., Zhang, B., Li, J., Zhao, J., 2017. Temporal and spatial changes of land use and landscape in a coal mining area in Xilingol grassland. IOP Conf. Ser. Earth Environ. Sci. 52, 012052. https://doi.org/10.1088/1742-6596/52/1/012052

Joshi, P.K., Kumar, M., Midha, N., Yanand, V., Wal, A.P., 2006. Assessing areas deforested by coal mining activities through satellite remote sensing images and gis in parts of Korba, Chattisgarh. J. Indian Soc. Remote Sens. 34, 415–421. https://doi.org/10.1007/BF02990926

Katakey, B.P., 2021. One Man Commission of Inquiry, Vol I. Guwahati.

Khan, I., Javed, A., 2012. Spatio-Temporal Land Cover Dynamics in Open Cast Coal Mine Area of Singrauli, M.P., India. J. Geogr. Inf. Syst. 04, 521–529. https://doi.org/10.4236/jgis.2012.46057

Kiran, S., Kumar, R., Gogoi, K., 2022. Land Use/Land Cover Dynamics During 2001 And 2021 Using Google Earth Engine and GIS in Ramagundam Coal Mining Area, A Part of Pranhita Godavari Valley, Southern India. J. Sci. Res. 66, 63–68. https://doi.org/10.37398/JSR.2022.660107

Kumar, M., Srivastava, M.K., Kishor, K., Singh, A.K., 2023. An Assessment of the Environmental Impact of Coal Mining through Acid Mine Drainage and Soil Degradation from Makum Coalfields, Upper Assam, India: A Case Study. J. Geol. Soc. India 99, 1113–1120. https://doi.org/10.1007/s12594-023-2437-3

Kutir, C., Agblorti, S.K.M., Campion, B.B., 2022. Migration and Estuarine Land Use/Land Cover (LULC) Change along Ghana's Coast. Reg. Stud. Mar. Sci. 54, 102488. https://doi.org/10.1016/j.rsma.2022.102488

Lin, B., Wang, Y., Wang, H., Xiao, W., 2021. Quantifying the Impacts of Coal Mining and Soil-Water Conservation on Runoff in a Typical Watershed on the Loess Plateau, China. Water 13, 3229. https://doi.org/10.3390/w13223229

Liu, Y., Liu, R., Chen, J., Wei, X., Qi, L., Zhao, L., 2024. A global annual fractional tree cover dataset during 2000–2021 generated from realigned MODIS seasonal data. Sci. Data 11, 832. https://doi.org/10.1038/s41597-024-03671-9

López-Bedoya, P.A., Bohada-Murillo, M., Ángel-Vallejo, M.C., Audino, L.D., Davis, A.L. V., Gurr, G., Noriega, J.A., 2022. Primary forest loss and degradation reduces biodiversity and ecosystem functioning: A global meta-analysis using dung beetles as an indicator taxon. J. Appl. Ecol. 59, 1572–1585. https://doi.org/10.1111/1365-2664.14167

Łowicki, D., 2008. Land use changes in Poland during transformation. Landsc. Urban Plan. 87, 279–288. https://doi.org/10.1016/j.landurbplan.2008.06.010

Mishra, A., Swamy, S.L., Thakur, T.K., Kumar, A., Pandey, M., 2022. Impact of coal mining on land use changes, deforestation, biomass, and C losses in Central India: Implications for offsetting CO 2 emissions. L. Degrad. Dev. 33, 3731–3747. https://doi.org/10.1002/ldr.4419

Mishra, M., Santos, C.A.G., Nascimento, T.V.M. do, Dash, M.K., Silva, R.M.D., Kar, D., Acharyya, T., 2022. Mining impacts on forest cover change in a tropical forest using remote sensing and spatial information from 2001-2019: A case study of Odisha (India). J. Environ. Manage. 302. https://doi.org/https://doi.org/10.1016/j.jenvman.2021.114067

Mishra, P.K., Rai, A., Rai, S.C., 2020. Land use and land cover change detection using geospatial techniques in the Sikkim Himalaya, India. Egypt. J. Remote Sens. Sp. Sci. 23, 133–143. https://doi.org/10.1016/j.ejrs.2019.02.001

Mohanty, B., Mohanty, P., Mahalik, G., 2020. Effect of Coal Mining on Vegetation of Talcher Area of Odisha, India. Int. J. Mod. Agric. 9, 325–331.

Nedd, R., Light, K., Owens, M., James, N., Johnson, E., Anandhi, A., 2021. A Synthesis of Land Use/Land Cover Studies: Definitions, Classification Systems, Meta-Studies, Challenges and Knowledge Gaps on a Global Landscape. Land 10, 994. https://doi.org/10.3390/land10090994

Niyonsenga, J., Sibomana, E., 2024. The Impact of Mining Activities on Land Use and Land Cover Change in Rwamagana District, the Case of Muhazi Sector, Rwanda. J. Agric. 8. https://doi.org/10.53819/81018102t2419

Okoduwa, A.K., Amaechi, C.F., Enuneku, A.A., 2025. Assessing Land Use/Land Cover and Predicting Future Scenarios in Kano Metropolis, Northern Nigeria. Jordan J. Earth Environ. Sci. 16, 267–275.

Pandey, P.C., Koutsias, N., Petropoulos, G.P., Srivastava, P.K., Ben Dor, E., 2021. Land use/land cover in view of earth observation: data sources, input dimensions, and classifiers—a review of the state of the art. Geocarto Int. 36, 957–988. https://doi.org/10.1080/10106049.2019.1629647

Patra, T., Duttaa, D., Kundu, A., Kumar, M., Hossain, S.S., Chattoraj, K.K., 2022. Evolution of Opencast Mines in the Raniganj Coalfield (India): An Assessment through Multi-temporal Satellite Data. J. Geol. Soc. India 98, 387–394. https://doi.org/10.1007/s12594-022-1990-5

Ranjan, A.K., Parida, B.R., 2019. Paddy acreage mapping and yield prediction using sentinel-based optical and SAR data in Sahibganj district, Jharkhand (India). Spat. Inf. Res. 27, 399–410. https://doi.org/10.1007/s41324-019-00246-4

Ranjan, A.K., Sahoo, D., Gorai, A.K., 2021. Quantitative assessment of landscape transformation due to coal mining activity using earth observation satellite data in Jharsuguda coal mining region, Odisha, India. Environ. Dev. Sustain. 23, 4484–4499. https://doi.org/10.1007/s10668-020-00784-0

Tamfuh, P.A., Musi, E.N., Fils, S.C.N., Ateh, K.I., Aye, A.B., Tata, E., Mamdem, L.E., Kenzong, B., Nono, G.D.K., Bitom, D., 2024. Mapping Land use/Land Cover Changes Caused by Mining Activities from 2018 to 2022 Using Sentinel-2 Imagery in Bétaré-Oya (East-Cameroon). J. Geosci. Geomatics 12, 12–23. https://doi.org/10.12691/jgg-12-1-3

Thakur, T.K., Dutta, J., Upadhyay, P., Patel, D.K., Thakur, A., Kumar, M., Kumar, A., 2022. Assessment of land degradation and restoration in coal mines of central India: A time series analysis. Ecol. Eng. 175, 106493. https://doi.org/10.1016/j.ecoleng.2021.106493

Trautwein, C., Pletterbauer, F., 2018. Land Use, in: Riverine Ecosystem Management. Springer International Publishing, Cham, pp. 241–252. https://doi.org/10.1007/978-3-319-73250-3_13

Uddin Siddiqui, A., Kumar Jain, M., 2022. Change analysis in land use land cover due to surface mining in Jharia coalfield through Landsat time series data. Mater. Today Proc. 49, 3462–3468. https://doi.org/10.1016/j.matpr.2021.04.277

Vieira, S.M., Kaymak, U., Sousa, J.M.C., 2010. Cohen's kappa coefficient as a performance measure for feature selection, in: International Conference on Fuzzy Systems. IEEE, pp. 1–8. https://doi.org/10.1109/FUZZY.2010.5584447

Yadav, S., Kumar, A., Raj, H., Bora, H.R., 2018. Lichen diversity in coal mining affected areas of Makum coalfield, Magherita, Assam. Trop. Plant Res. 5, 243–249. https://doi.org/10.22271/tpr.2018.v5.i2.031